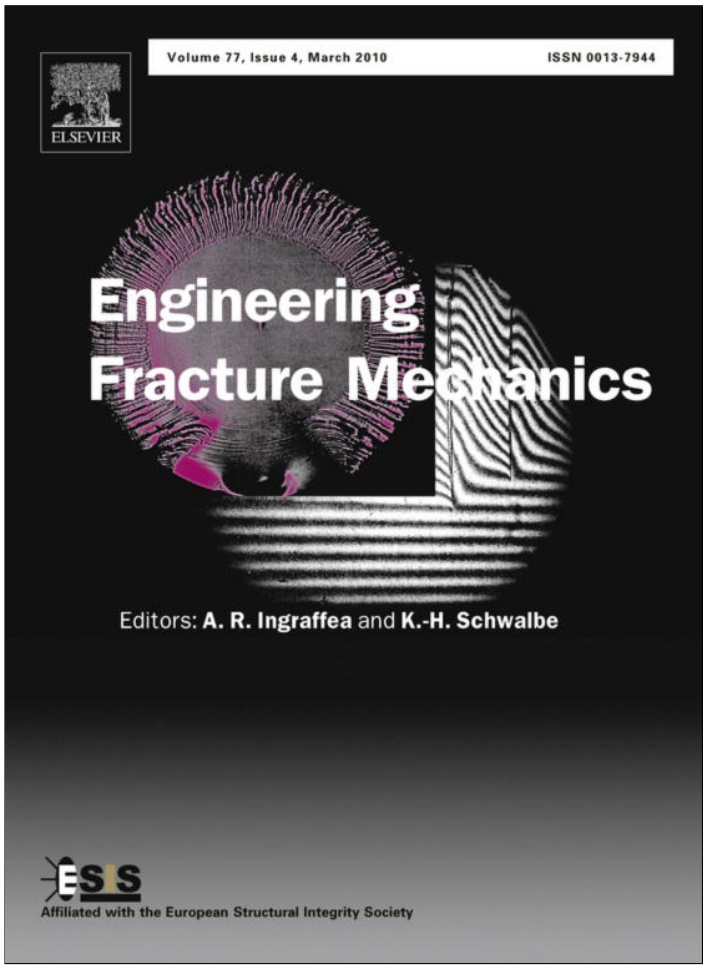

Engineering Fracture Mechanics 77 (2010) 631–645

Contents lists available at ScienceDirect

Engineering Fracture Mechanics

journal homepage: www.elsevier.com/locate/engfracmech

Experiments and predictions of the effects of load history on cleavage fracture in steel

D.J. Smith [a,*], S. Hadidi-Moud [c], A.H. Mahmoudi [d,1], A. Mirzaee Sisan [b], C.E. Truman [a]

[a] Solid Mechanics Research Group, Department of Mechanical Engineering, University of Bristol, Bristol BS8 1TR, UK
[b] DNV Energy, Palace House, London SE1 9DE, UK
[c] Ferdowsi University of Mashad, Mashad, Iran
[d] Director of Residual Stresses Laboratory, Mechanical Engineering Department, University of Bu-Ali Sina, Hamedan, Iran

ARTICLE INFO

Article history:
Received 11 January 2009
Received in revised form 29 October 2009
Accepted 28 November 2009
Available online 2 December 2009

Keywords:
Interaction
Residual stress
WPS
Local compression
FE
Local approach

ABSTRACT

A series of experiments conducted on two steels, A533B and A508, are summarised. Tests were conducted to explore the influence of different room temperature pre-loading cycles on subsequent low temperature (−150 °C and −170 °C) cleavage fracture. In all cases the low temperature fracture toughness was modified, with tensile pre-loading increasing the toughness and precompression reducing the toughness.

Results from finite element simulation of the pre-loading cycles are illustrated. Tensile pre-loading created compressive residual stresses and precompression generated tensile residual stresses. The residual stresses were adopted in a stress based local approach to fracture model using Weibull statistics and applied to the experimental results. The parameters in the Weibull model were calibrated for the virgin steels prior to its application to prior loading cases. The model is found to be successful in predicting the change in toughness relative to the virgin material for pre-loading in tension of A533B steel. The model underestimated the change in toughness for tensile pre-loading of A508 steel and overestimated the toughness change for precompression of both steels.

1. Introduction

Prior loading influences the fracture and fatigue response of many metallic materials [1]. In particular, there is extensive experimental data illustrating that prior loading changes the subsequent fracture response of many steels exhibiting cleavage fracture at low temperature [2–9]. Prior loading events such as proof loading and warm pre-stressing result in a rather significant improvement in "apparent" low temperature cleavage fracture toughness of ferritic steel structures. This is provided prior loading is in the same direction as the final loading to fracture [10]. Recent evidence together with numerical analysis has shown that local crack tip residual stresses are principally responsible for these effects [7,8]. Additional factors include changing material behaviour through prior straining and introduction of crack tip blunting [4,5].

Cleavage fracture toughness has a statistical variation [11,12]. Smith and Booker [13] illustrate that this statistical variation is modified when the material has been subjected to prior load events. Experimental evidence, summarised by Smith and Booker [13], shows that if the prior loading (at room temperature) is in the same direction as the final low temperature fracture there is an increase in the mean toughness together with an increase in the shape parameter (or Weibull modulus) compared to the virgin material. These changes are only apparent if there is sufficient constraint to plastic flow during the

* Corresponding author. Tel.: +44 1173315913.
E-mail address: david.smith@bristol.ac.uk (D.J. Smith).
[1] Tel.: +98 (811) 825 7410; fax: +98 (811) 825 7400.

0013-7944/$ - see front matter © 2009 Elsevier Ltd. All rights reserved.
doi:10.1016/j.engfracmech.2009.11.016

prior loading. Alternatively, if the prior loading is compressive statistical evidence reveals a reduction in the mean toughness and the shape parameter.

Methods for predicting the effects of prior load history can be generally classed as "toughness-based" and "stress-based" [13]. The former is derived from early work by Chell [2] and Smith and Garwood [3] to predict change in toughness following in-plane prior loading and even for events that simulate thermal shock loading [14]. The "toughness-based" method was not intended to take account of statistical variations but nevertheless attempts have been developed to predict statistical variations using a Monte Carlo simulation [13] or alternatively modifying the failure probability curve for the virgin material [15].

The "stress-based" method uses the local stresses near to the crack tip to predict the onset of cleavage fracture. This is commonly termed the local approach to fracture (LAF) recently reviewed in detail by Pineau [12,16]. The term LAF refers generally to a comprehensive range of local models, usually based on Weibull statistics, with or without the influence of plastic strain. Overall, the LAF technique relies on using finite element analysis to determine the local stress and or the strain fields. This is then incorporated into a statistical model that predicts the probability of failure for the onset of cleavage fracture. The LAF models have also been used to predict how prior load events change probability of failure and was first considered by Beremin [17] and explored further by Hadidi-moud et al. [9], Yuritzinn et al. [14] and Lefevre et al. [18]. The application of a stress based local approach model is explored further in this paper.

The paper follows a series of recent papers [1,8,9,13] and theses [19,20] by the authors similarly examining the effects of prior load on fracture particularly in the context of near crack tip residual stresses created through prior loading. The primary purpose of this paper is to assess the ability of a model using the local approach to fracture to predict the observed fracture behaviour of steels that have been subjected to single and multiple prior loading paths. The paper first summarises recent experimental results [19,20]. The experiments are then examined using elastic–plastic finite element analysis to provide an understanding of how local crack tip events change during the loading history. Results from this analysis are subsequently used to predict the failure probability of cleavage fracture after prior loading. These predictions are then compared with experimental results.

2. Experiments

Experimental results were obtained from two pressure vessel steels, A533B and A508. A series of experiments were conducted using a variety of temperature and loading cycles, illustrated in Figs. 1 and 2. Conventional fracture toughness tests were conducted on steels in their as-received (or virgin) condition using a simple cool and fracture (CF) cycle, Fig. 1a. All tests

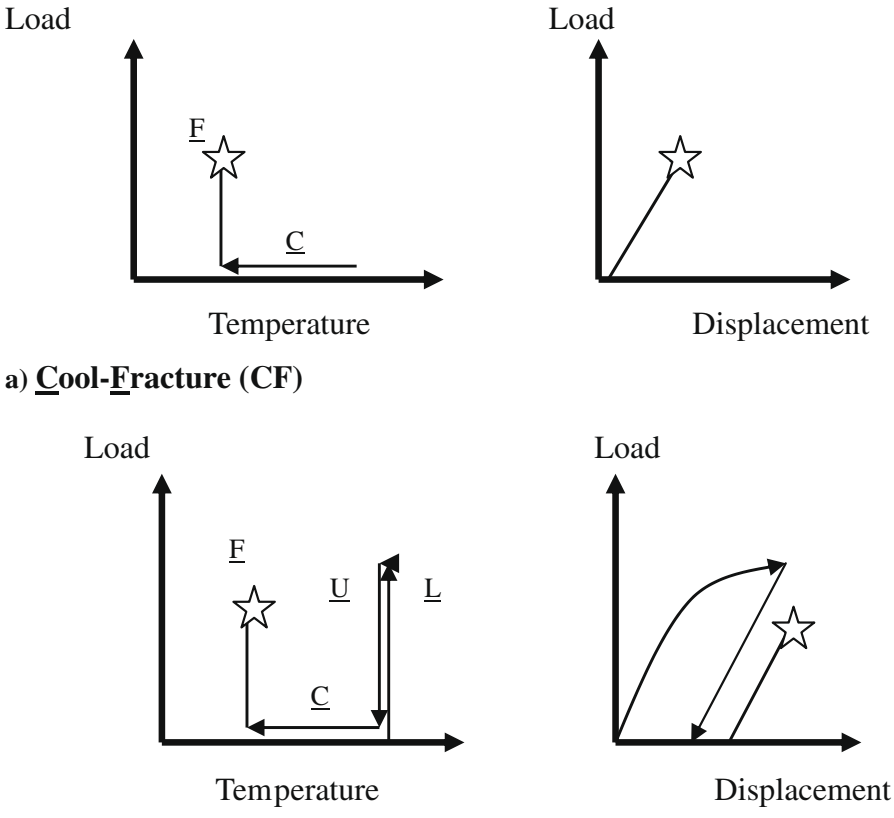

Fig. 1. Load and temperature cycles CF and LUCF.

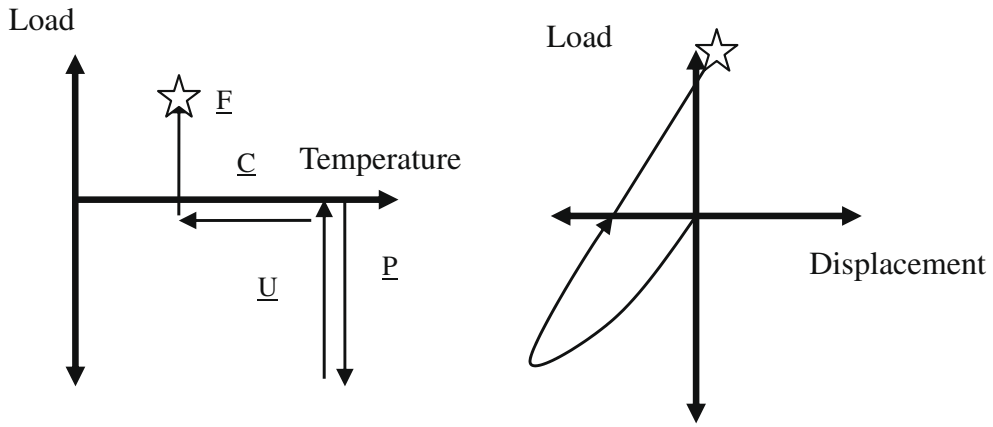

a) Punch-Unload-Cool-Fracture (PUCF) or Compress-Unload-Cool-Fracture (CUCF)

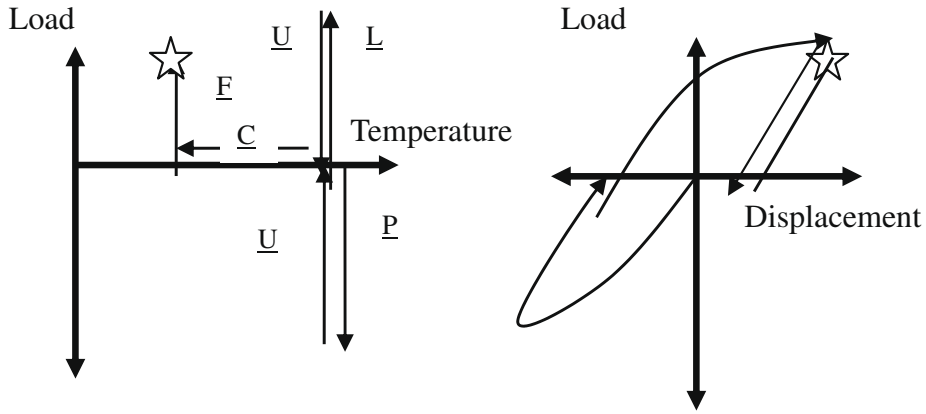

b) Punch-Unload-Load-Unload-Cool-Fracture (PULUCF)

Fig. 2. Load and temperature cycles PUCF, CUCF and PULUCF.

were conducted at temperatures where failure was cleavage fracture. A load-temperature cycle, often denoted as LUCF, [1] has been commonly been used to study the effects of warm pre-stressing on cleavage fracture, Fig. 1b. Here the tensile prior loading or in-plane loading and unloading, at room temperature, was in the same direction as the load leading to final fracture.

Alternatives to tensile in-plane loading include local out-of-plane compression [19,21,22] and in-plane compression [20,23]. For the purposes of this paper the former is classified as the PUCF cycle and the latter denoted as the CUCF cycle, Fig. 2a. Both cycles were performed on selected specimens. Finally, multiple pre-loading cycles, denoted as the PULUCF cycle, Fig. 2b, were performed.

For the two steels the variability of the failure loads was determined by usually undertaking 10 or more tests for each test condition. The fracture toughness, K, was determined from the maximum load at fracture using standard formulae [24] and the cumulative probability for all tests was determined from

$$P_f = \frac{i - 0.5}{N} \tag{1}$$

where N and i are the total number of specimens and the order number, respectively.

2.1. A533B steel

Load history tests on two sets of A533B steel have been reported earlier. Set 1 consists of CF and LUCF tests conducted by Smith and Garwood [6]. Tests were conducted using 50 mm thick single edge notch bend, SEN(B) specimens with the fracture temperature at −170 °C and the prior loading at room temperature (20 °C). In all cases the crack length to width ratio, a/W, was 0.5. In these tests the specimens were fatigue pre-cracked prior to any loading cycle. Set 2 are results provided by Mirzaee-Sisan et al. [20,23] for CF and PUCF tests using 25 mm thick compact tension C(T) specimens, $a/W = 0.5$, tested at −170 °C. The PUCF cycle was achieved by subjecting C(T) specimens to out-of-plane compression [19,23]. This was done by applying compression to the sides of the C(T) specimen using 25 mm diameter hardened steel punches. Compressive loading was sufficient to reduce permanently the specimen thickness by about 2%.

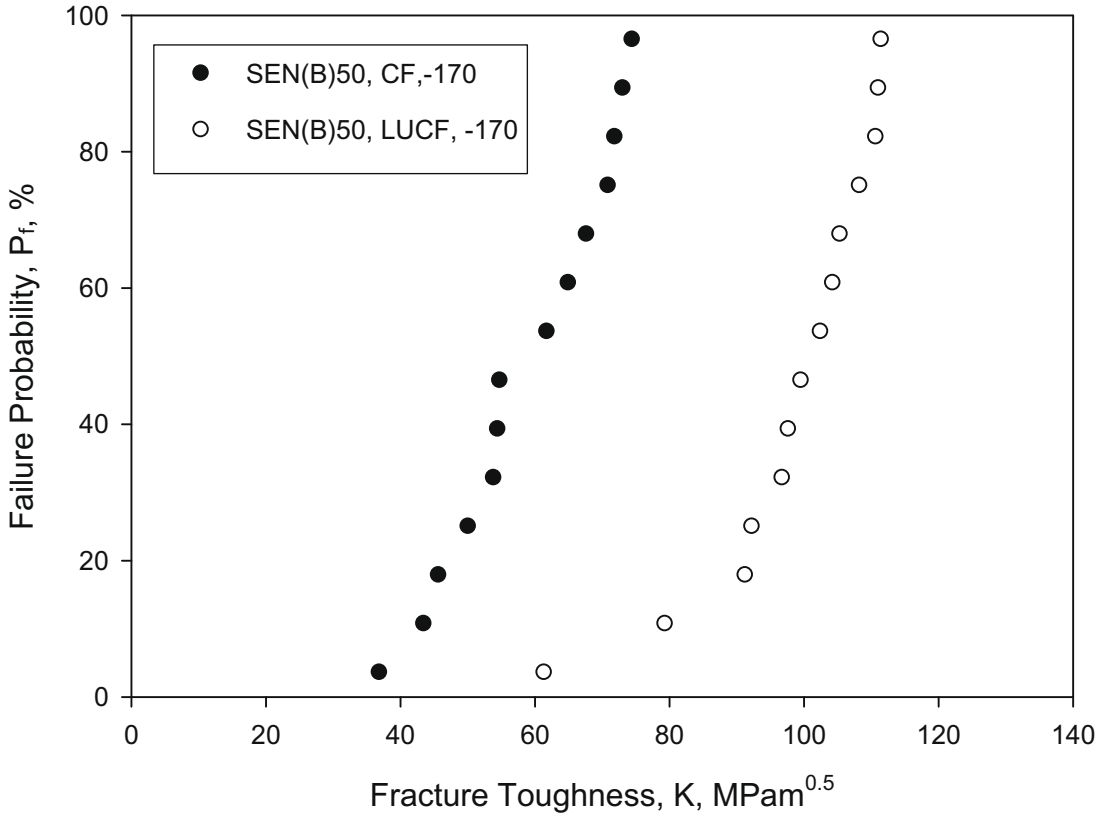

Fig. 3. Experimental results for A533B steel for CF and LUCF tests at −170 °C.

In this second set of A533B steel tests Mirzaee-Sisan et al. [20,23] also conducted tests using the CUCF cycle applied to 10 mm thick SEN(B) specimens with $a/W = 0.3$. The in-plane compression and unload parts of the cycle were conducted on notched SEN(B) specimens. The specimens were then electro-discharge machined (EDM) to introduce sharp notches, 0.1 mm radius. This was prior to the cooling to −150 °C and final reloading to fracture. These tests were compared to SEN(B) specimens containing 0.1 mm radius EDM notches subjected to a CF loading cycle.

A summary of experimental results for both sets of A533B are shown in Figs. 3 and 4 with results for set 1 in Fig. 3 and set 2 measurements illustrated in Fig. 4. Statistical analysis of these results has been reported by Smith and Booker [13].

It is evident from Fig. 3 that the LUCF loading cycle introduces changes that enhance the as-received fracture toughness. These results were examined by Hadidi-moud et al. [9] to explore the application of a local approach for predicting fracture after prior loading. In contrast, an out-of-plane (PUCF) and an in-plane (CUCF) prior compressive cycle resulted in a reduction in fracture toughness compared with the as-received toughness as shown in Fig. 4, with the CUCF cycle reducing the toughness more than PUCF cycle.

2.2. A508 steel

Experiments were carried out [19] to measure the change in toughness of A508 steel resulting from prior loading. Tests were carried out using 25 mm thick C(T) specimens with $a/W = 0.5$ subjected to CF, LUCF, PUCF and PULUCF cycles. In all cases the final fracture temperature was −170 °C with all prior loading cycles conducted at 20 °C.

The LUCF and PUCF tests were similar to those conducted on A533B steel. The PU and LU load cycles were conducted at room temperature. The cycle was completed by cooling to −170 °C and loading to fracture. The load level for LU part of the full PULUCF cycle was identical to that used in the LUCF tests.

Experimental results for these various loading cycles are illustrated in Fig. 5. As with the results for A533B steel the LUCF cycle considerably enhanced the fracture toughness of A508 steel. The PUCF cycle reduced the as-received toughness. Finally, the PULUCF cycle enhanced the toughness to a similar level to that for the LUCF cycle. Consequently, the loading history created during the out-of-plane compression did not appear to modify the benefit created by the LUCF cycle alone.

3. Finite element studies

One purpose of the finite element (FE) studies was to provide insight to the details of the crack tip stress fields created by the various loading and temperature cycles used in the experimental programme. A second purpose of the FE analysis was to use the stresses created at each stage of the loading cycle for subsequent prediction of failure. This is described later.

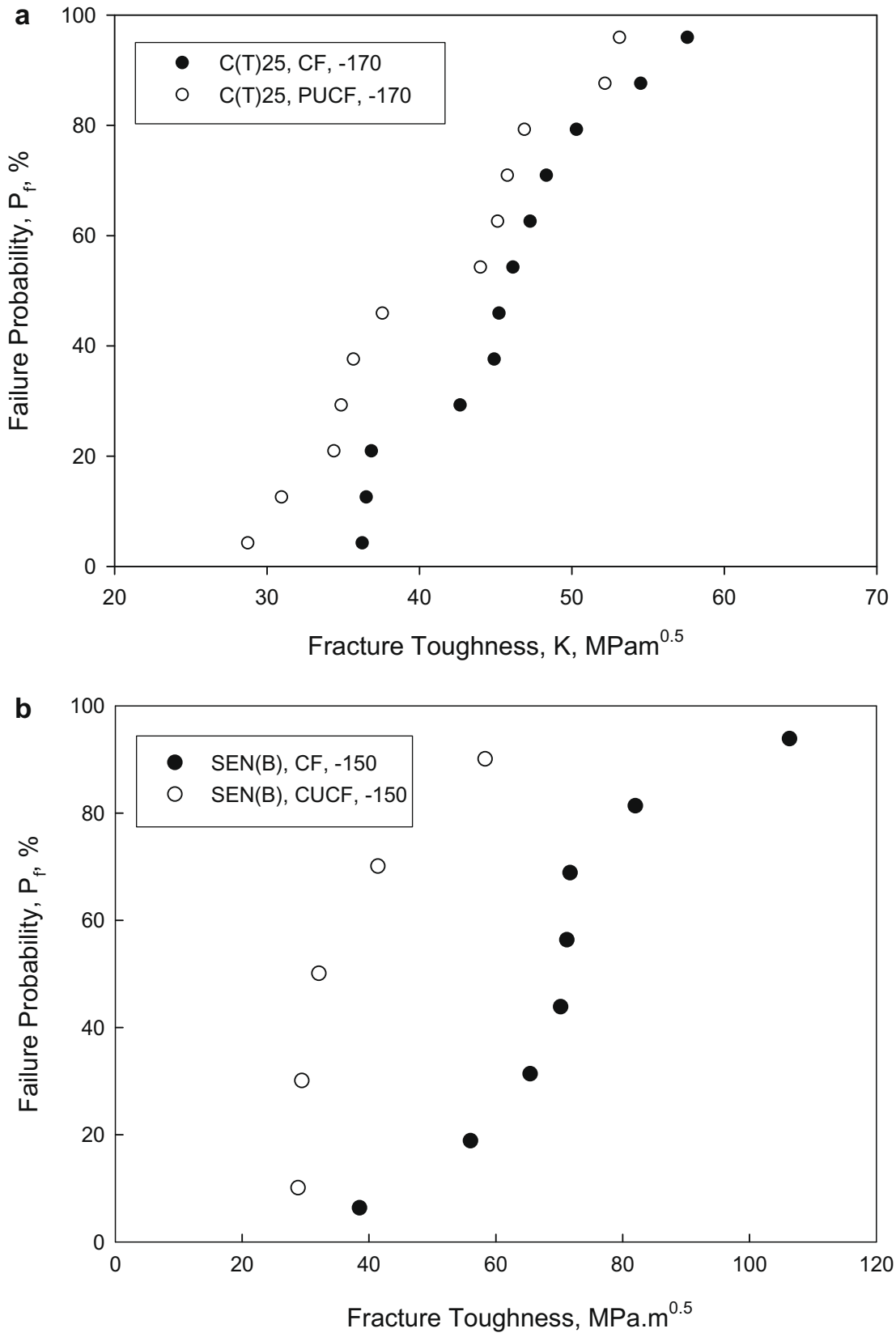

Fig. 4. Experimental results for A533B steel: (a) CF and PUCF tests using C(T)25 specimens at −170 °C, (b) CF and CUCF tests using SEN(B)10 specimens at −150 °C.

All the FE analyses in this paper were conducted using three-dimensional (3-D) models of both SEN(B) and C(T) specimens using 8-noded quadrilateral reduced integration elements. One quarter models were created using ABAQUS/CAE [25]. In the crack tip region the mesh was refined to a degree that the element size normal to the crack front and in the

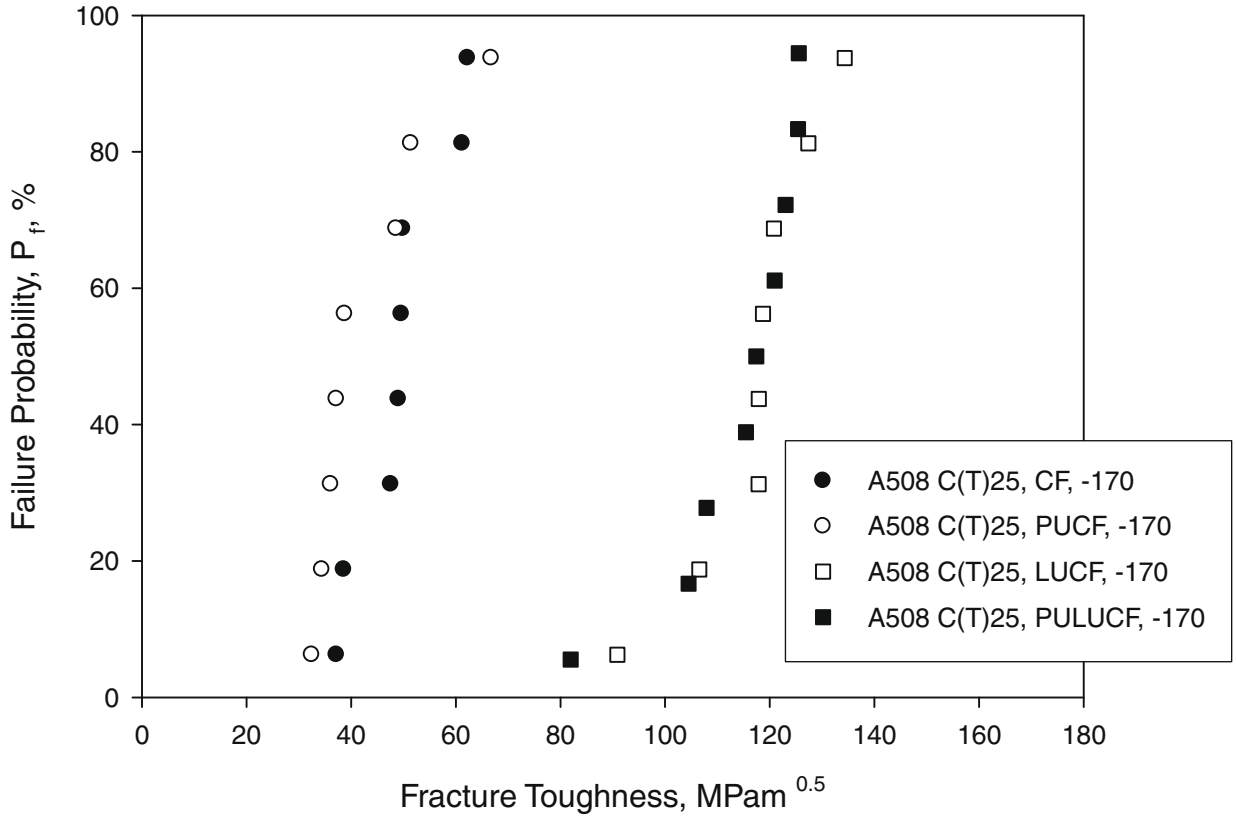

Fig. 5. Experimental results for A508 steel subjected to CF, PUCF, LUCF and PULUCF load cycles using C(T)25 specimens at −170 °C.

direction of crack propagation was 0.025 mm. Also in general the models had 16 layers of elements in their thickness direction and therefore the element size in the through thickness direction was about 0.78 mm.

A number of material models were used including isotropic, kinematic and mixed hardening models [8,19,20]. For example, earlier work [8] demonstrated that details of the material hardening model, such as the Bauschinger effect, had a significant influence on the details of the local residual stresses generated during the prior loading cycle. However, when subsequently reloaded at the low temperature the material model did not significantly change the predictions of fracture. Consequently, for both steels (A533B and A508) post yield response was assumed to be isotropic hardening.

3.1. Simulation of loading cycles

The CF and LUCF cycles were simulated using the same techniques described elsewhere [8,9]. For the pre-loading and unloading part of the LUCF cycle the appropriate room temperature elastic–plastic properties were adopted for both steels. This process simulated blunting of the crack tip and creation of near crack tip residual stresses as a consequence of local plastic strains being accommodated in an unloaded elastic stress field. The material properties were then transformed from room temperature values to their low temperature values in one step. Consequently the residual stresses were allowed to redistribute prior to reloading at the lower temperature. Reloading in the FE analysis was continued to loads corresponding to those observed in the experiments.

For each steel the process of subjecting the sample to out-of-plane compression at room temperature in the PUCF cycle was first simulated. Since a one quarter model was used it was only necessary to model a single 25 mm diameter cylindrical punch tool with its centre positioned over on the line of the crack, with the edge of the tool over the crack tip. The position of the punch tool was decided based on the results of a parametric study [21] and provided the most tensile residual stresses near to the crack tip. Appropriate boundary conditions and contact properties were applied and the simulation of out-of-plane compression was carried out in two stages. In the first stage the punching tool was moved towards the specimen and impressed the punch into the surface. Frictionless contact [19,21] between the faces of the rigid punching tool and the specimen was assumed. After the punch and unload portion (PU) of the cycle the remaining cool and fracture portion (CF) was the same as for the LUCF cycle.

The PULUCF cycle was simulated only for the A508 steel. The analysis was carried using a combination of the various loading cases. The punching then unloading cycle, followed by reload and unload (PULU) conditions were simulated at 20 °C. As before the final fracture was assumed to occur at −170 °C and therefore the low temperature properties were imposed. Reloading was then applied to a load corresponding to the appropriate experimental fracture load.

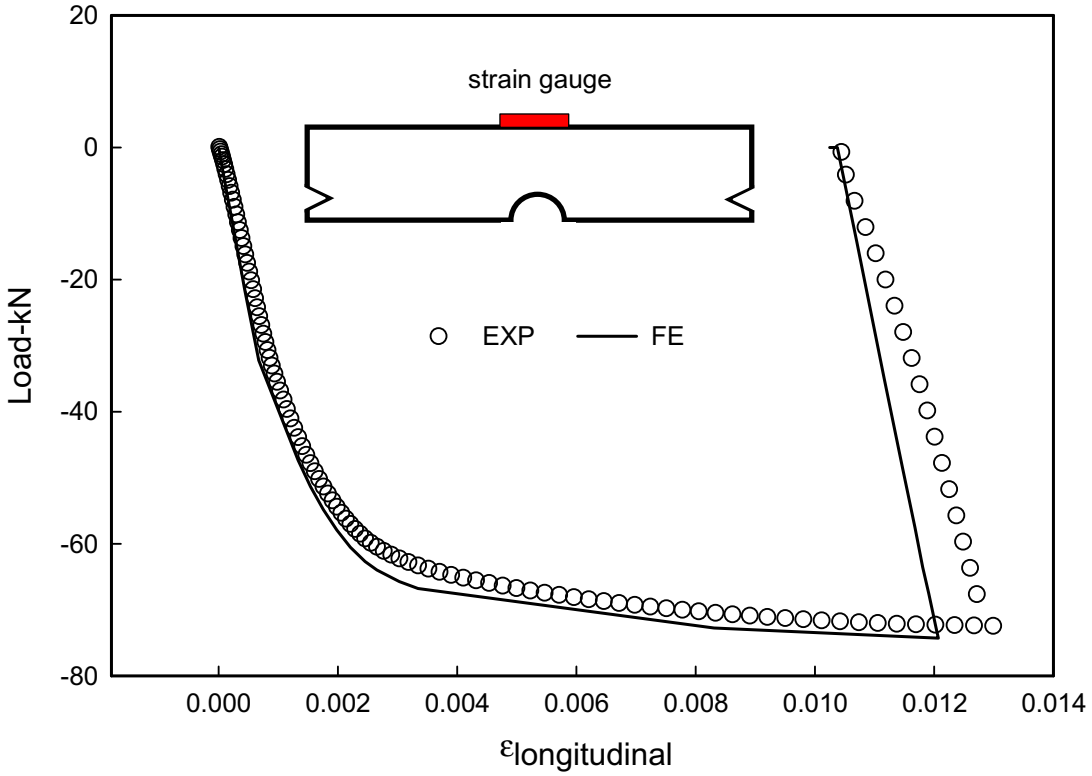

Fig. 6. Variation of longitudinal back-face strain on a SEN(B) specimen during compression pre-loading.

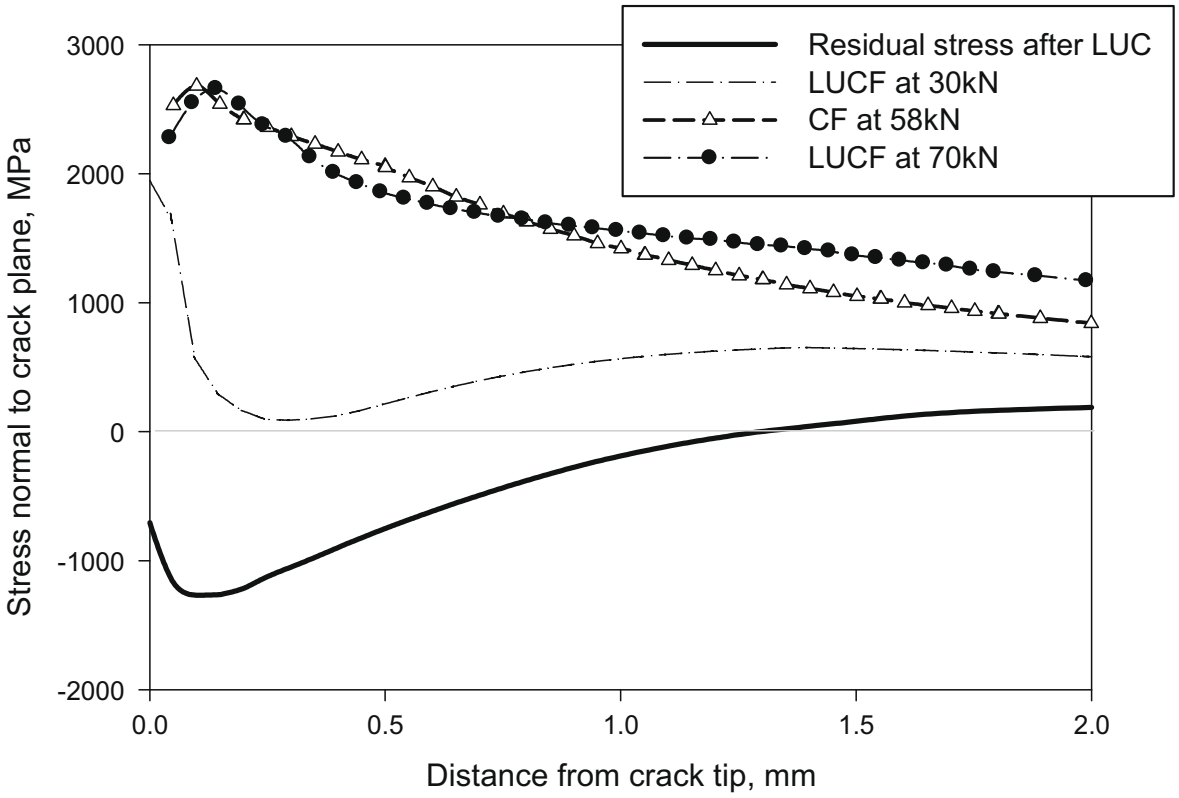

Fig. 7. Distribution of normal to the crack plane stresses in a SEN(B)50 specimen of A533B steel at −170 °C.

To mimic the experiments the CUCF cycle was simulated for the A533B steel, first by subjecting a notched SEN(B) specimen to in-plane compression [20,23]. A typical result is shown in Fig. 6 where the applied compressive load and back-face strains are compared with experimental results. After unloading a notch of 0.1 mm was introduced by incrementally

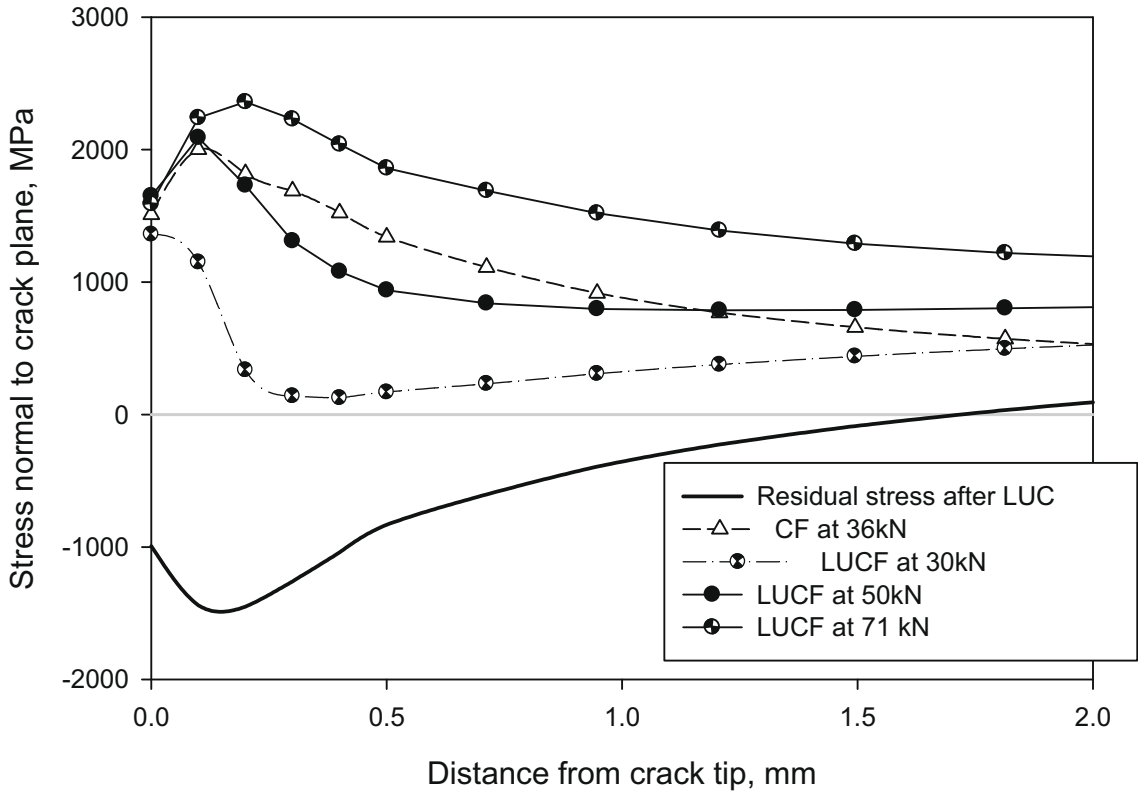

Fig. 8. Distribution of normal to the crack plane stresses in a C(T)25 specimen of A508 steel at −170 °C.

removing elements to simulate the EDM process carried out in the experiments. In this case the crack was introduced after establishing the residual stresses and the initial residual stress field was redistributed.

3.2. Near crack tip stresses

It is assumed that in the model for the local approach to fracture (LAF) the maximum principal stress normal to the crack plane, σ_1, is the controlling parameter. This is presented in more detail later in the paper. It is instructive therefore to examine the nature of the distributed stress, σ_1, ahead of the crack tip at different stages of the various loading cycles examined in the experimental programme. Typical results from the FE analysis have been selected and are shown in Figs. 7–11. The results correspond to stress distributions directly ahead of the crack tip at the centre of the thickness of a specimen.

3.2.1. Simple cool-fracture, CF, cycle

The reference analysis for comparison with all load histories is the CF simulation where no load history was assumed and the cracked specimen was loaded from its virgin state until fracture at the cleavage fracture temperature. For example, Figs. 7 and 8 show the stress normal to the crack plane obtained for an A533B steel SEN(B)50 specimen and an A508 steel C(T)25 specimen, both fractured at −170 °C. In the case of the SEN(B)50 specimen the stress distribution corresponds to a fracture load of 58 kN, while for the A508 steel C(T)25 specimen the distribution relates to a fracture load of 30 kN.

3.2.2. Load-unload-cool-fracture, LUCF, cycle

Stresses were extracted from the FE simulations at different stages in the LUCF cycle. For example Figs. 7 and 8 shows compressive stress distributions immediately after loading, unloading and then cooling (LUC) prior to reloading to fracture. A sufficient level of pre-loading at room temperature, at which the material response is ductile and undergoes significant plastic deformation prior to fracture, results in the formation of a relatively extended plastic zone around the crack front, thus leaving a "local" residual stress field after unloading. In both steels the region of compressive stresses extends to about 1.5 mm ahead of the crack tip. On reloading at low temperature it can be seen that at certain values of low or moderate load levels the stresses remain rather lower than those obtained in the CF analysis. However, eventually when the applied load is sufficiently high the local maximum principal stress matches the stress field corresponding to the CF case. Fig. 7 illustrates that a final applied load of 70 kN is required in the LUCF case compared to a load of 50 kN for the CF condition. Similar results are shown for an A508 steel C(T)25 specimen in Fig. 8.

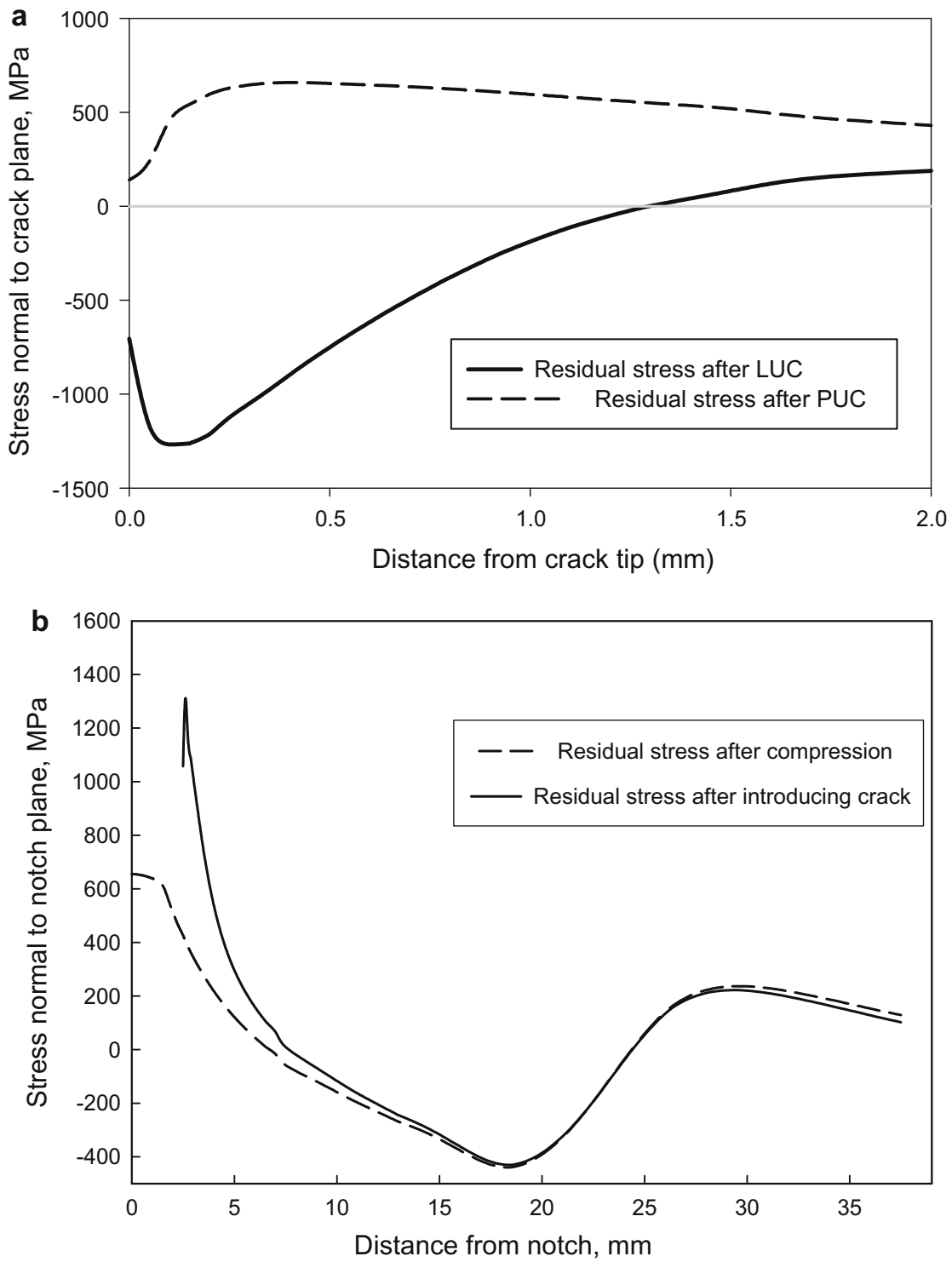

Fig. 9. Distribution of normal to the crack plane stresses: (a) in a C(T)25 specimen of A508 steel at −170 °C for two different prior load histories, (b) in a notched SEN(B)10 specimen of A533B steel at −150 °C after precompression with and without a crack. The crack was introduced incrementally by removing elements.

3.2.3. Compressive pre-loading, PUCF and CUCF cycles

In contrast to pre-loading in tension and unloading as in the LUCF cycle the pre-loading elements of the PUCF and CUCF cycles introduce tensile residual stresses ahead of the crack tip. This is demonstrated in Figs. 9 and 10. In the case of an A508 steel C(T)25 specimen subjected to an out-of-plane precompression, or the PUC elements of the PUCF cycle, Fig. 9a illustrates that the residual stresses are tensile for distances in excess of 2 mm ahead of the crack tip. In contrast, pre-loading in tension provided compressive stresses of higher magnitude than the tensile residual stresses. However the compressive residual stresses were confined to a smaller distance ahead of the crack tip.

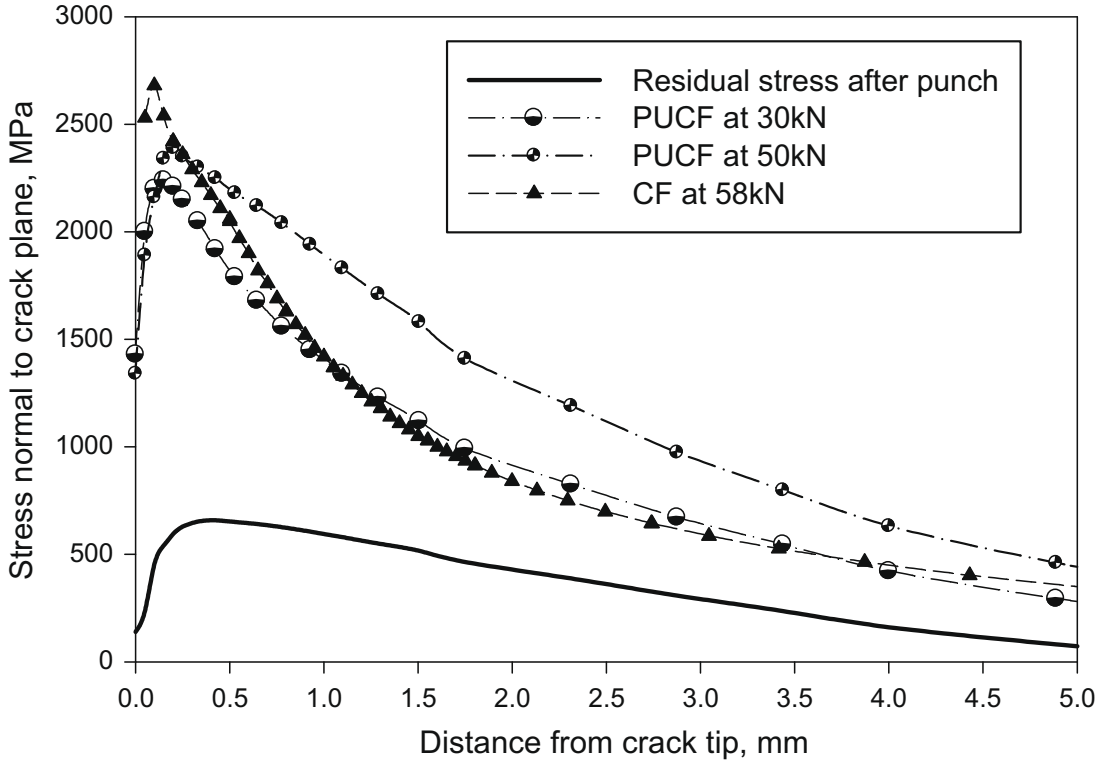

Fig. 10. Distribution of normal to the crack plane stresses in a C(T)25 specimen of A508 steel at −170 °C.

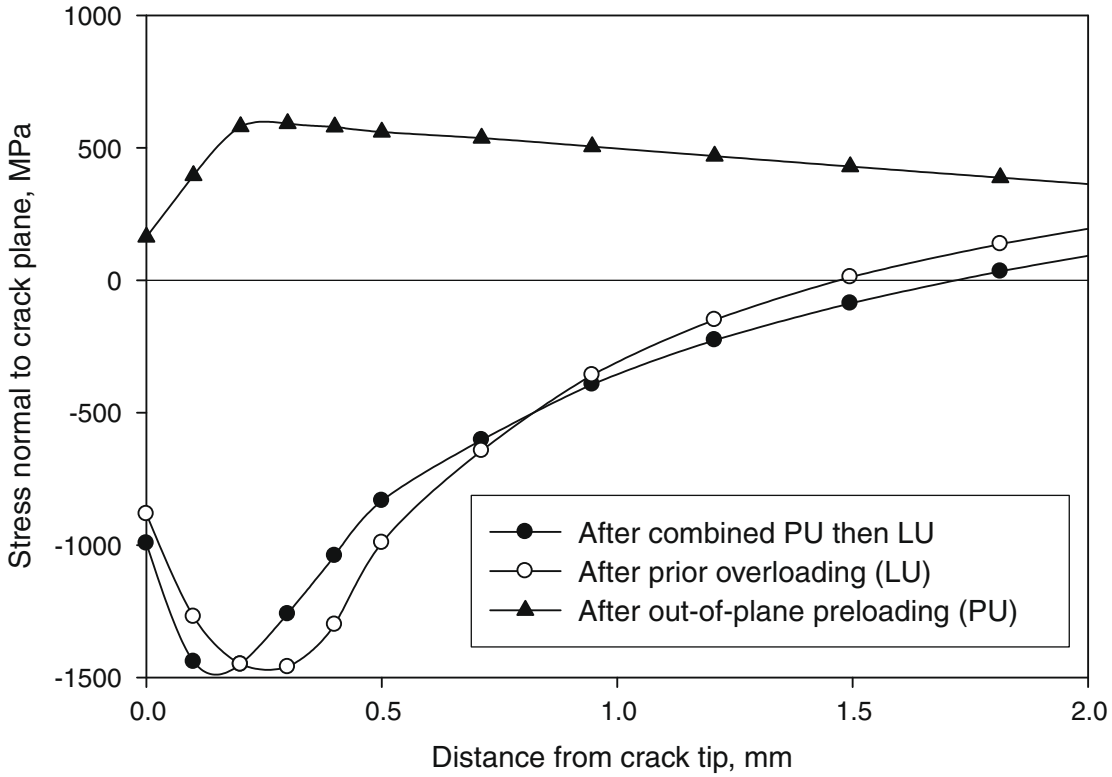

Fig. 11. Distribution of normal to the crack plane stresses in a C(T)25 specimen of A508 steel at −170 °C subjected to PU, LU and PULU cycles.

In the case of the in-plane precompressed notched SEN(B)10 specimen the region of the tensile residual stress ahead of the notch was substantial. Fig. 9b shows a tensile region was created for distances up to 7 mm ahead of the notch tip. The FE simulation of incrementally introducing the 0.1 mm radius EDM notch further elevated the peak tensile residual stresses.

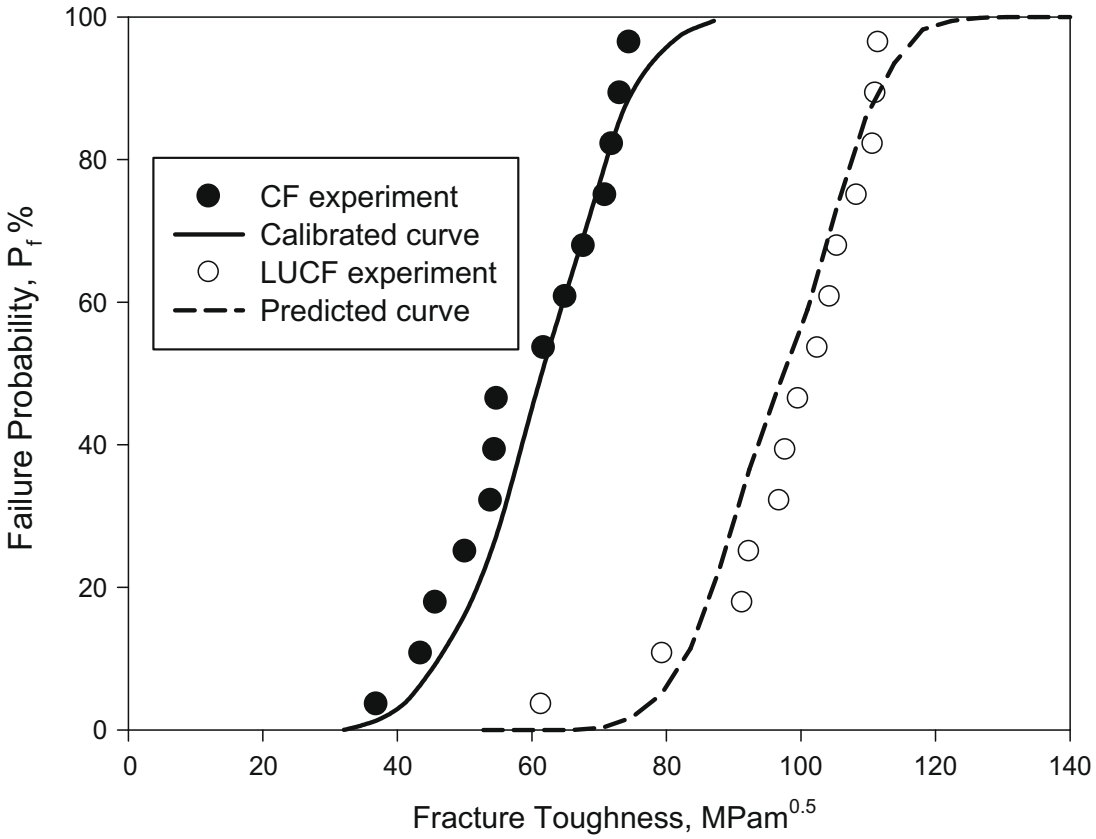

Fig. 12. Comparison of predicted and measured toughness of LUCF experiments conducted on A533B steel at −170 °C using SEN(B)50 specimens.

Maximum principal stress distributions corresponding to the reloading conditions (i.e. the PUCF cycle) at low temperature for an A508 steel C(T)25 specimen are shown in Fig. 10. Also shown is the stress distribution for a CF cycle for a failure load of 58 kN. It can be seen that at a load of 30 kN in the PUCF cycle the stress distribution approximately matched that of the CF cycle at 58 kN, although not the peak stress. A further increase in load in the PUCF cycle to 50 kN also did not produce the necessary increase in peak stress. However, the stresses at this load substantially increased above the CF condition for distance in excess of 0.5 mm ahead of the crack tip.

3.2.4. Multiple pre-loadings, PULUCF cycles

Finally it is helpful to illustrate stress distributions corresponding to multiple pre-loading. Results are shown in Fig. 11. Similar to Fig. 9a, the maximum principal stress corresponding to out-of-plane compressive (PU) pre-loading and in-plane tensile pre-loading (LU) are shown. The former pre-loading (PU) created a tensile residual stress field and the tensile pre-loading formed compressive residual stresses. When a previously PU preloaded C(T) sample was subsequently subjected to a LU cycle (to form the PULU cycle) the resulting residual stress field is similar to the LU cycle as shown in Fig. 11. Nevertheless there are some differences. Notably the position of the peak compressive stress ahead of the crack tip after PULU is greater than for the LU case.

4. Prediction of failure probability

4.1. Methodology

To predict failure probability after pre-loading a Beremin type [12,16,17] model was adopted and follows the methodology adopted in earlier work by Hadidi-moud et al. [9]. It is assumed that the local failure probability, $P_f[\sigma_w]$, is based on the local Weibull stress and is given by

$$P_f[\sigma_w] = 1 - Exp\left[-\left\{\frac{\sigma_w - \sigma_{\min}}{\sigma_u - \sigma_{\min}}\right\}\right]^m \tag{2}$$

where $\sigma_{\min}$ is a threshold stress, σ_u is a characteristic stress, m is a Weibull modulus and σ_w is the Weibull stress given by:

$$\sigma_w = \left[\frac{1}{V_0}\int_{V_p}\sigma_1^m dV\right]^{\frac{1}{m}} \tag{3}$$

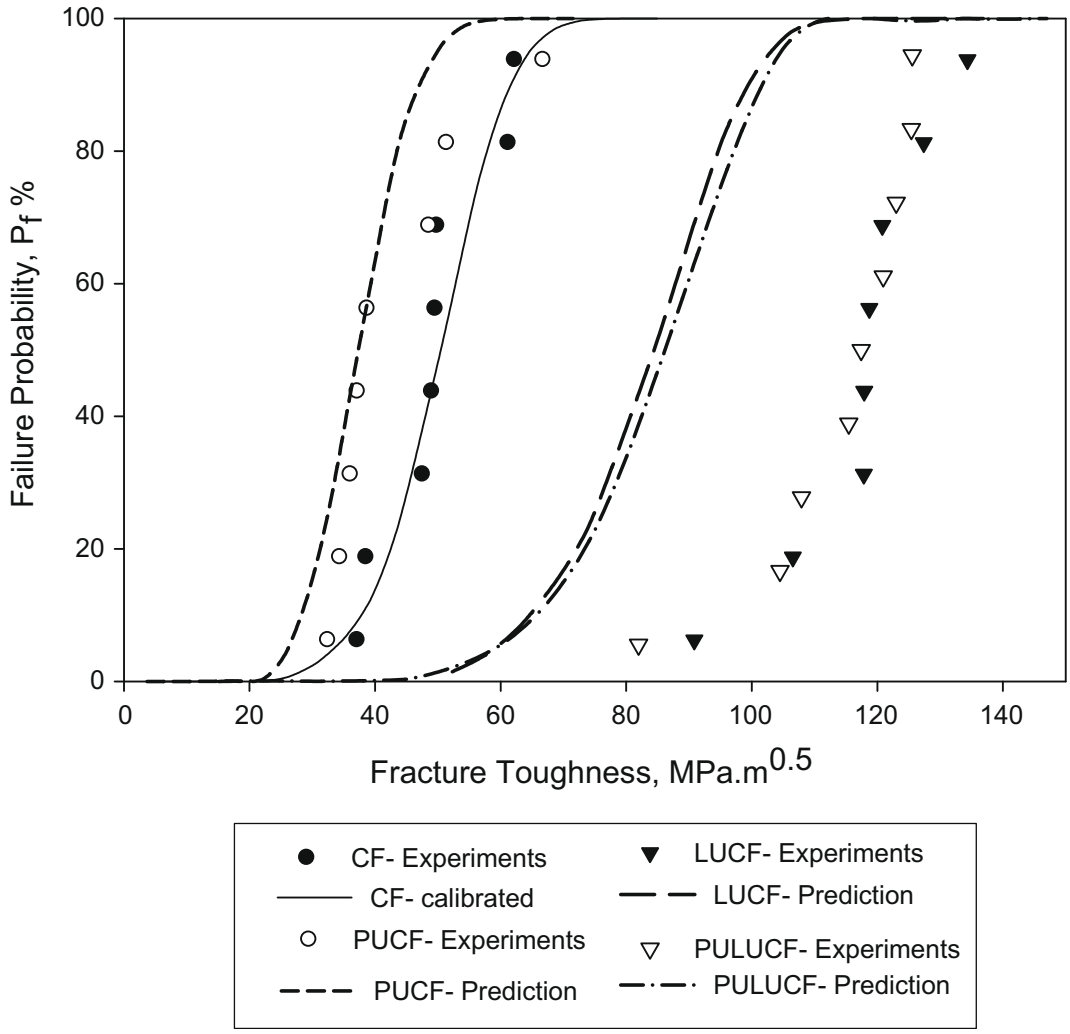

Fig. 13. Comparison of predicted and measured fracture toughness of LUCF, PUCF and PULUCF experiments conducted on A508 steel at −170 °C using C(T)25 specimens.

where V_0 is a reference volume, V_p is the near crack tip active plastic volume, and σ_1 is the maximum principal stress within the plastic volume.

The information required from the finite element analysis to examine the local approach to fracture therefore included identification of the crack tip active plastic volume, V_p as well as the maximum principal stresses at all integration points of the elements contained within V_p. Notably, since 3D FE analyses were conducted all elements along and ahead of the crack front and within the active plastic volume were examined. Here, the active plastic volume refers to plasticity created on reloading and ignores the influence of plasticity developed during pre-loading. A user routine was developed to obtain stresses from the FE analysis and then to calculate failure probabilities using Eqs. (2) and (3). Therefore, for a specific material and specimen geometry subjected to a known remote applied load the failure probability was determined. The applied load also corresponded to an applied stress intensity factor, K and consequently each load analysis created a pair of values of P_f and K.

This analysis required knowledge of the parameters, $\sigma_{\min}$, σ_u, m and V_0, all of which are interdependent [26]. Following earlier work [9,23] m and V_0 were selected as being equal to 4 and 0.01mm^3 respectively, and the remaining parameters determined by selecting values that gave the best fit to the experimental data for the virgin material (i.e. the CF loading condition). Curves corresponding to the best fit parameters for the CF condition for the two steels are shown in Figs. 12–15. The Weibull parameters are given in Table 1.

Having determined the Weibull parameters the next stage was to determine failure probabilities after prior loading events. It was assumed that prior loading did not modify the parameters and there was no associated (and accumulated) failure probability from the prior load sequence. It was therefore supposed that the sole purpose of the prior loading sequence was to introduce an initial stress state. The stresses, as a consequence of subsequent reloading, within a reactivated plastic volume, were then used in the analysis. The results derived from this analysis are described next.

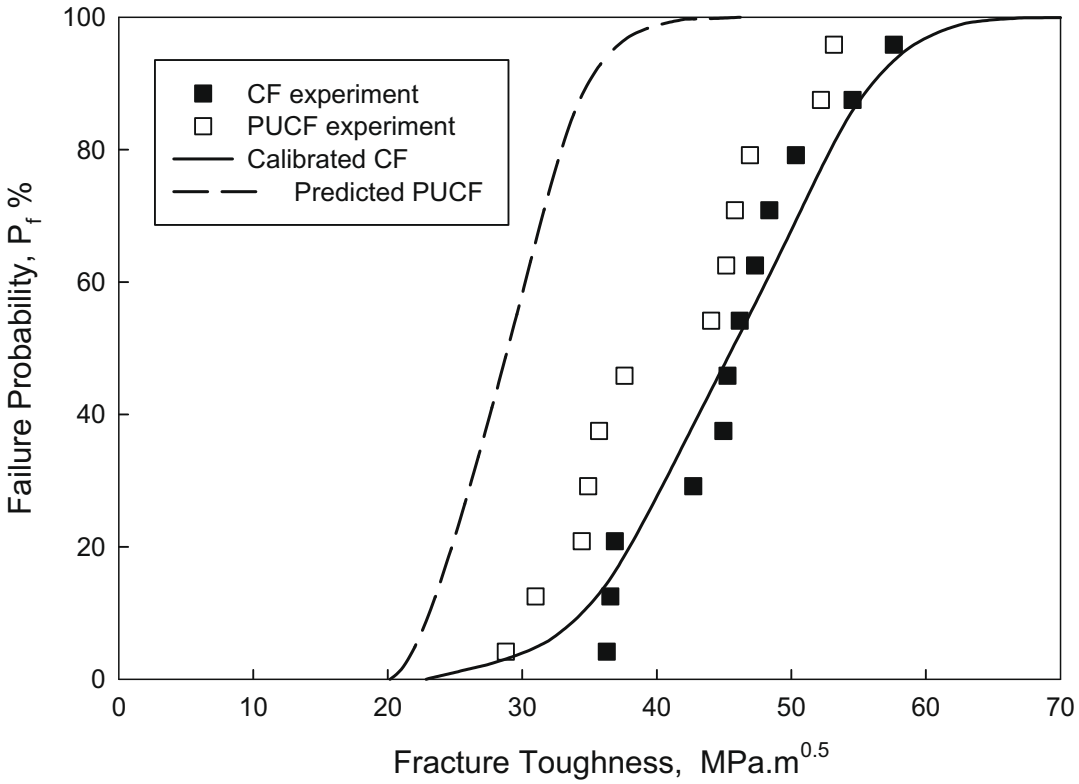

Fig. 14. Comparison of predicted and measured toughness for PUCF experiments conducted on A533B steel at −170 °C using C(T)25 specimens.

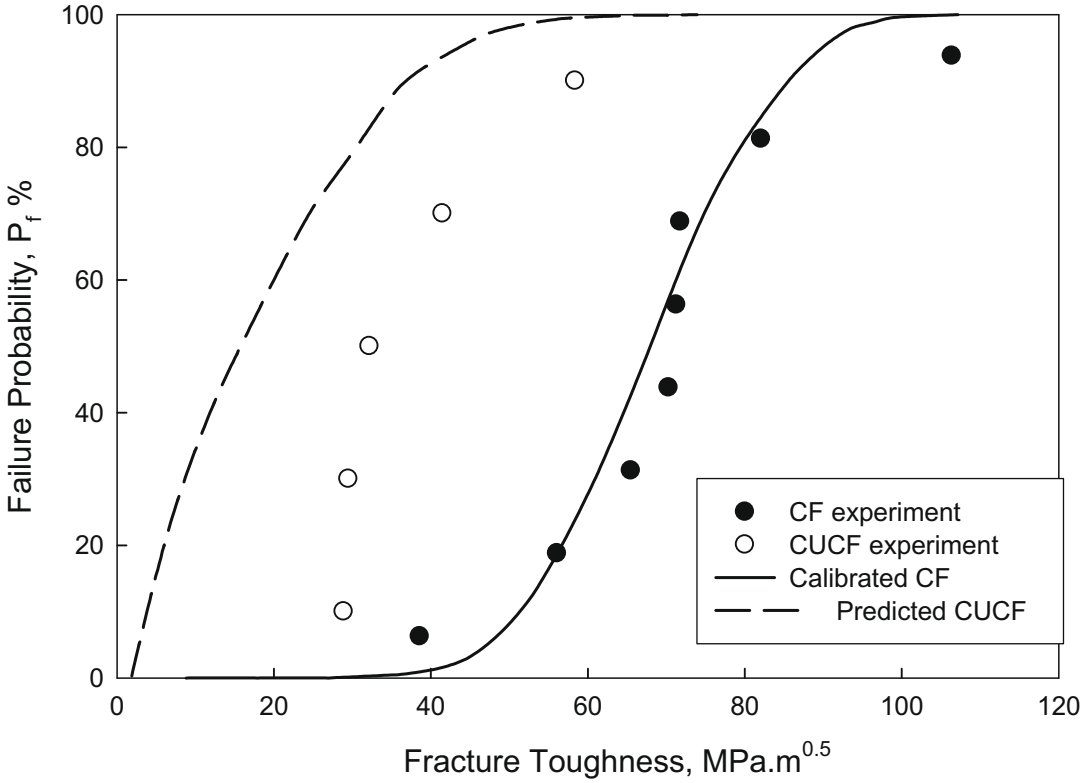

Fig. 15. Comparison of prediction and measured toughness following in-plane loading CUCF for A553B steel SEN(B)10 specimens fractured at −150 °C.

4.2. Predictions for preloaded states

For the LUCF cycle the predicted failure probability curves for the A533B and A508 steels are shown in Figs. 12 and 13. In the case of the A533B steel the predicted curve agrees well with the LUCF experimental results and reproduces the results

Table 1
Weibull parameters used for probability distributions for A533B and A508 steels.

Steel in AR condition, specimen type, test temperature (°C)	Assumed shape parameter, m	Assumed reference volume, V_0 (mm^2)	Characteristic stress, σ_u (GPa)	Threshold stress, σ_{min} (GPa)
A533B set 1 SEN(B), −170	4.0	0.01	7.25	4.0
A533B set 2 C(T), −170	4.0	0.01	7.9	2.85
A533B set 2 SEN(B), −150	4.0	0.01	10	2.85
A508, C(T), −170	4.0	0.01	9.0	3.0

given earlier by Hadidi-moud et al. [9]. In contrast for the A508 steel the LUCF prediction considerably underestimates the LUCF test results and suggests other factors not included in the analysis contribute to the increased toughness observed in the A508 steel experiments.

Turning to the predictions for the PUCF and CUCF cycles, Figs. 13–15 show that the model predicts reductions in fracture toughness for both load cases compared with the material in its virgin condition. The observed reduction in the experimental toughness in the A508 and A533B steels, Figs. 13 and 14 respectively, after the PUCF cycle was found by Smith and Booker [13] to be statistically inconclusive when compared to the virgin state. Notably, the predicted reduction in toughness for the A508 steel, Fig. 13, was broadly similar to the experiments and would also be treated as statistically insignificant. In contrast the predicted distribution for A553B steel, shown in Fig. 14, is statistically significant.

Experimental data corresponding to the CUCF cycle was sparse but nonetheless illustrated a reduction in toughness after in-plane precompression compared to the virgin (CF) state. The model also predicted a reduction in toughness but to values less than observed.

The predicted failure probability distribution determined from using the multiple pre-loading cycles created in the PU-LUCF condition is shown in Fig. 13. This distribution is very similar to the LUCF prediction for this steel. However, as with the LUCF experiments, the predicted toughness for a given failure probability is lower than the toughness from the PULUCF experiments for the same probability.

5. Discussion

The experiments and predictions presented in this paper reveal two important characteristics about the influence of prior loading on cleavage fracture in steels. The first feature is that experimentally, both steels illustrate similar fracture characteristics when subjected to prior loading. Notably pre-loading in a direction identical to the lower temperature reloading resulted in an increased fracture toughness. This is emphasised by results shown in Figs. 3 and 5. In a detailed statistical analysis of this data and various other fracture data for the LUCF cycle Smith and Booker [13] found that in all cases the increase was statistically significant as defined through F and t-tests [27]. In contrast the PUCF cycles, i.e. out-of-plane precompression, reduced the cleavage fracture toughness (Figs. 4a and 5), but, as pointed out by Smith and Booker [13], these reductions were not statistically significant. When pre-loading, through in-plane compression, CUCF, is introduced, experimental results revealed a greater reduction in the toughness. However there were not a sufficient data to undertake F and t-tests. The more complex loading cycles in the PULUCF revealed that the most important influence on toughness is provided ultimately by the cycle undertaken just prior to final cooling and loading to fracture.

The second characteristic is that the predictions provided by the model utilised in this paper are neither more robust nor less convincing in providing statistical predictions than those offered by other routes [8,9,13]. The model proves to be successful for the LUCF results for A533B steel SEN(B)50 specimens shown in Fig. 12 but it is of limited success for the remaining cases. For example, the model was unable to capture the substantial increase in toughness for the A508 steel subjected to an LUCF and PULUCF cycles. When applied to the in-plane or out-of-plane precompression (PUCF or CUCF) cycles the model overestimated the reductions in toughness compared to the experiments. Nevertheless, it is apparent that in all applications of the LAF model the predictions either underestimate the improvement in toughness or overestimate the reduction in toughness.An underlying feature of the model used in this paper is that the parameters derived from the as-received toughness can be used to predict the toughness after a prior loading event. In this paper, the parameters m and V_0 were fixed and σ_{min} and σ_u determined so as to fit the CF experimental data. Such an approach was also adopted with moderate success by Hadidi-moud et al. [9] when considering prior load effects (LUCF) on different specimen shapes. Notably, for each geometry, the Weibull parameters were fitted directly to data for the same geometry in the CF or virgin condition. It was argued that a change in the Weibull modulus reflected a change in geometry and indirectly a change in the stress triaxiality, so that for a notched bar the parameter m was larger than for a sharp tipped crack created in a C(T) or SEN(B) specimen. The outcomes of the earlier study also suggested that a prior loading event did not change substantially the local triaxiality.

The model adopts Weibull expressions (Eqs. (2) and (3)) incorporating maximum principal stress and the active plastic volume as the governing parameters. As Pineau [16] points out LAF models should consider nucleation of microcracks with the onset of plastic deformation and remain active over the loading history. More recently, it has been suggested that the effect of plastic strain can be included into LAF models, [28,29], to accommodate both continuous nucleation of microcracks and blunting of already initiated microcracks. However, these recent studies have been focussed on predicting failure taking account of plastic strain during loading to final failure, particularly for changes in constraint (or triaxiality), [29]. There is

considerable merit in considering whether such modifications to LAF models are suitable for variable loading histories as discussed by Lefevre et al. [18]. It could be assumed that the LU part of the LUCF loading cycle blunted microcracks. Consequently, there would be an additional increase in toughness above that predicted by the model considered in this paper. This is observed for the A508 steel C(T)25 specimens shown on Fig. 15. The potential of blunted microcracks may also contribute to the results revealed after the PUCF and CUCF loading cases. Here the predicted toughness reduction as a consequence of the presence of tensile residual stresses, as illustrated in Figs. 9 and 10 was lower than observed suggesting that the reduction was ameliorated by an additional factor.

6. Conclusions

A series of experiments conducted on two steels, A533B and A508, using a C(T) and SEN(B) specimens, revealed that prior loading cycles conducted at room temperature, modified the load bearing capacity for cleavage fracture at low temperatures (-150 °C and -170 °C). In-plane tensile pre-loading increased the toughness. In-plane and out-of-plane precompression reduced the toughness.

Simulations of the pre-loading cycles, using finite element analysis, revealed the generation of compressive residual stresses for the case of tensile pre-loading and conversely, tensile residual stresses for precompression. Using parameters derived from specimens not subjected to prior loading, together with the residual stresses following pre-loading, a local approach to fracture model predicted changes in toughness. The model was moderately successful. In one case, LUCF cycle applied to A533B steel, the model correctly predicted the change. In all other cases, LUCF applied to A508, PUCF, CUCF and PULUCF, the predictions were overestimated for precompression cycles and underestimated for tensile reloading.

References

[1] Smith DJ. The influence of prior loading on structural integrity. In: Ainsworth RA, Schwalbe KH, editors. Comprehensive structural integrity, vol. 7. Amsterdam: Elsevier; 2003. p. 289–345.
[2] Chell GG. Some fracture mechanics applications of warm pre-stressing to pressure vessels. In: Proc 4th int conf pres ves technol, I. Mech E; 1980. p. 117–24.
[3] Smith DJ, Garwood SJ. The significance of prior overload on fracture resistance: a critical review. Int J Press Ves Pip 1990;41:255–96.
[4] Reed PAS, Knott JF. Investigation of the role of residual stress in the warm pre-stress (WPS) effect part I – experimental. Fatigue Fract Engng Mater Struct 1996;19(4):485–500.
[5] Reed PAS, Knott JF. Investigation of the role of residual stress in the warm pre-stress (WPS) effect part II-analysis. Fatigue Fract Engng Mater Struct 1996;19(4):501–13.
[6] Smith DJ, Garwood SJ. Experimental study of effects of prior overload on fracture toughness of A533B steel. Int J Press Ves Pip 1990;41:297–331.
[7] Smith DJ, Hadidi-moud S, Fowler H. The effects of warm pre-stressing on cleavage fracture – part 1 evaluation of experiments. Engng Fract Mech 2004;71(13–14):2015–32.
[8] Smith DJ, Hadidi-moud S, Fowler H. The effects of warm pre-stressing on cleavage fracture - part 2 finite element analysis. Engng Fract Mech 2004;71(13–14):2033–51.
[9] Hadidi-Moud S, Mirzaee-Sisan A, Truman CE, Smith DJ. A local approach to cleavage fracture in ferritic steels following warm pre-stressing. Fatigue Fract Engng Mater Struct 2004;27:931–42.
[10] Burdekin FM, Lidbury DPG. Views of TAGSI on the current position with regards to benefits of warm prestressing. Int J Press Ves Pip 1999;76:885–90.
[11] Evans AG. Statistical aspects of cleavage fracture of steels. Met Trans A 1983;14A:1349–55.
[12] Pineau A. Practical application of local approach methods. In: Ainsworth RA, Schwalbe KH, editors. Comprehensive structural integrity, vol. 7. Amsterdam: Elsevier; 2003. p. 177–225.
[13] Smith DJ, Booker JD. Statistical analysis of the effects of prior load on fracture. Engng Fract Mech 2007;74:2148–67.
[14] Yuritzinn T, Ferry L, Chapuliot S, Mongabure P, Moinereau D, Dahl A, et al. Illustration of the WPS benefit through BATMAN test series: tests on large specimens under WPS loading configurations. Engng Fract Mech 2008;75:2191–207.
[15] Lewis S, Truman CE, Smith DJ. A comparison of 2D and 3D fracture assessments in the presence of residual stresses. In: Proceedings of the ASME pressure vessels and piping conference, San Antonio, Texas, USA; 2007 [CD].
[16] Pineau A. Development of the local approach to fracture over the past 25 years: theory and applications. Int J Fract 2006;138:139–66.
[17] Beremin FM. Numerical modelling of warm pre-stress effect using a damage function for cleavage fracture. In: Proceedings of 5th international conference on fracture, ICF5, vol. 2. Oxford Pregamon; 1981.
[18] Lefevre W, Barbier G, Masson R, Rousselier G. A modified Beremin model to simulate the warm pre-stress effect. Nucl Engng Des 2002;216:27–42.
[19] Mahmoudi AH. Influence of residual stresses on fracture. PhD thesis, University of Bristol, UK; 2005.
[20] Mirzaee-Sisan AH. The influence of prior thermal and mechanical loading on fracture. PhD thesis, University of Bristol, UK; 2005.
[21] Mahmoudi AH, Truman CE, Smith DJ. Using local out-of-plane compression (LOPC) to study the effects of residual stress on apparent fracture toughness. Engng Fract Mech 2008;75:1516–34.
[22] Mahmoudi AH, Stefanescu D, Hossain S, Truman CE, Smith DJ, Withers PJ. Measurement and prediction of the residual stress field generated by side-punching. ASME J Engng Mater Technol 2006;128:451–9.
[23] Mirzaee-Sisan A, Mahmoudi AH, Truman CE, Smith DJ. Application of the local approach to predict load history effects in ferritic steels. ASME pressure vessels and piping conference, PVP, Denver, Colorado, USA; 2005 (Paper 2005-71606).
[24] Anderson TL. Fracture mechanics, fundamentals and applications. CRC Press; 1995.
[25] Hibbit, Karlsson, Sorenson Inc. ABAQUS standard/ABAQUS-CAE users manuals. 1080 Main Street, Pawtucket, RI 02680-4847, USA: HKS Inc.; 2002.
[26] Gao X, Ruggieri C, Dodds RH. Calibration of Weibull stress parameters using fracture toughness data. Int J Fract 1998;92:175–200.
[27] Dieter GE. Engineering design: a materials and processing approach. 3rd ed. NY: McGraw-Hill; 2000.
[28] Bordet SR, Kartensen AD, Knowles DM, Wiesner CS. A new statistical local criterion for cleavage fracture in steel. Part 1 – model presentation. Engng Fract Mech 2005;72:435–52.
[29] Hohe J, Friedmann V, Wenk J, Siegele D. Assessment of the role of micro defect nucleation in probabilistic modelling of cleavage fracture. Engng Fract Mech 2008;75:3306–27.